

APPLICATIONS OF VERTICAL ELECTRICAL SOUNDING AND GROUND MAGNETIC SURVEY FOR GROUNDWATER EXPLORATION IN THE AREA SURROUNDING TAIZ CITY, YEMEN

Amin N. Al kadasi

Dept. of Geology, Fac. of Appl. Science, Taiz University
alkadasi2000@yahoo.com

Received: 13/9/2015

Accepted: 27/10/2015

This study was carried out at Habeel Salman, Wadi Rudagah and Al Hawjalah sites located west, east and north of Taiz City, respectively. Fifteen vertical electrical sounding stations were conducted in the study area by using Schlumberger configuration while the ground magnetic survey was conducted at Al Hawjalah site which contains one of the groundwater well fields that provide the city by the water.

The results of this study indicates the existence of two groundwater aquifers, the shallow aquifer composed of quaternary deposits and weathered volcanics and the deep aquifer composed mainly of highly fractured volcanic rocks. During the Cenozoic, These aquifers are structurally controlled by intense faulting affecting the area due to the emplacement of Yemen volcanic group , the opening of the Red Sea and the Gulf of Aden which resulted in the formation of successive series of grabens and horsts.

INTRODUCTION

The water availability per capita in Yemen is 130 m³ per year (i.e. 10 % of the average for the Middle-East, and only 2 % of the world average per capita consumption) this means that the Yemen is one of the most water stressed countries in the region as well as in the world [1].

Due to the absence of any significant perennial sources of surface water, Yemen depends mainly on exploitation of groundwater which is taken from the shallow aquifers and increasingly from deeper aquifers. In large parts of Yemen, water from the shallow aquifer is abstracted as well over the recharge from the limited rainfall. Thus, pumping is substantially from the deep aquifers which are depleting rapidly. The shortage of water supply becomes chronic problem in Yemen and it may soon reach catastrophic levels [1]. This problem becomes more acute in Taiz City where the piped water is distributed only once every 60 days or more. This serious water supply challenge driven by the scarcity of water resources, rapid population growth, decreasing the rate of aquifer recharge

from rainfall due to uncontrolled human activity, misguided agricultural development and a lack of law enforcement to regulate water use.

The objective of the present work is to explore the available groundwater aquifers and provide information concerning the structural framework that contribute to groundwater occurrences in the studied area by using vertical electrical sounding (VES) and ground magnetic survey techniques.

Groundwater exploration in hard rock areas is a very difficult task since these rocks are generally considered as impermeable rocks except in areas where they are fractured or faulted. localized accumulations of groundwater may occur in hard rocks with secondary porosity acquired by faulting, jointing and weathering and the groundwater yield depends on the size of fractures and their interconnections. The VES technique has been widely used for groundwater exploration both in soft and hard rocks, because it is simple, cost effective, and powerful in determining the resistivity variations of the different subsurface layers. The magnetic method is an important tool to detect the upper surface of the basement and, indirectly, the thickness of the unconsolidated sedimentary cover.

The present study was carried out at three sites in Taiz city, named Habel Salman "SI", Wadi Rudagah "SII" and Al Hawjalah "SIII" (Fig. 1). These sites are located in the western, eastern and northern parts of Taiz City, respectively. The VES technique was conducted at the first (SI) and second (SII) sites whereas the detailed ground magnetic survey was conducted at the third site (SIII).

GEOLOGY AND TECTONIC SETTING OF THE AREA

The city of Taiz lies at the northern flank foot of the east-west trending escarpment of Jabal Sabir (Fig. 1) which rises directly to an elevation of about 3000 m above sea level. The city extends in the north, east, and west directions as well as in the south along the lower parts of Jabal Sabir itself. A number of successive moderate to rugged hills (with different heights) and incised narrow valleys flow northwards from the city for several tens of kilometers. Some of these wadis are structurally controlled. The studied area is covered by two lithologic units unconformably resting on the Precambrian basement. The two lithologic units are covered, in turn, by quaternary deposits, up to 70 m, thick. The lower lithologic unit is represented by a volcanic sequence related to the Tertiary Yemen Volcanics. It consists of a repetition of mafic and felsic

cycles consisting of lava flows and pyroclastic beds. The period of maximum volcanic activity is thought to fall in the range of 29 – 20 Ma and is related to the Afar mantle plume that impacted the Arabia-Africa area during the Oligocene and also partly related to the opening of the Red Sea and the Gulf of Aden. The other lithologic unit is represented by Gabal Saber granit unit which dissect the Yemen volcanic sequence during the Miocene period. The Saber granite forms a subrounded high relief mountainous mass located directly to the south of Taiz city. It is medium to coarse grains and ranges in composition from syno – to alkali granite. The quaternary deposits are generally unconsolidated, poorly sorted and composed of subrounded fragments, up to 30 × 20 cm, separated by fine- grained sandy to silty matrix.

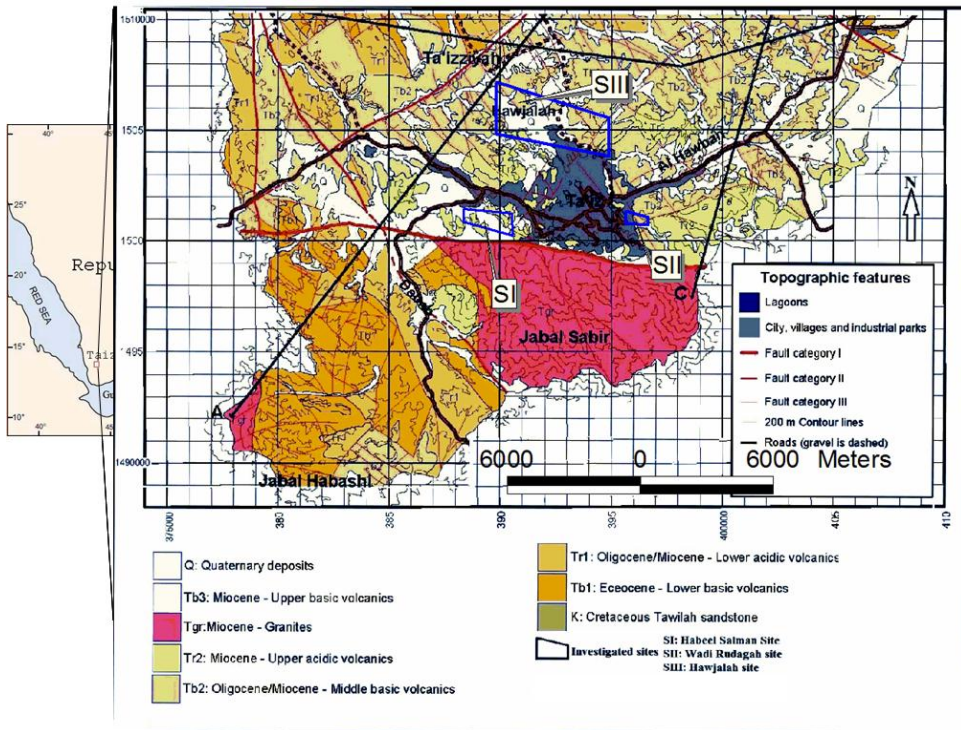


Figure 1: Location and geologic map of the study area (adapted from Dar El-Yemen [4]).

Tectonically, the exposed rocks in Taiz region reflect relics of the different tectonic events affected the whole Yemen as well as the Arabian Peninsula. The Precambrian time in Yemen is characterized by two tectonic trends, the oldest one is trending NE – SW, recognized south-east of Taiz region as a shear zone dissecting the Precambrian rocks, while the younger trend is represented by Najd fault system that trends NW in the

western part of Yemen and swinging to E-W in the eastern parts. During the Mesozoic several rift basins were formed through three separate phases of rifting during the Late Jurassic, associated with the fragmentation of Gondwana, then during Early to Mid-Cretaceous, related to the separation of India from Madagascar and finally during Cenozoic, associated with the opening of the Red Sea and the Gulf of Aden [8, 9, 10, 11 and 12]. Cenozoic NW-trending normal faulting (parallel to the Red Sea rift) affects both the sedimentary cover and the Yemen volcanics in the western part of Yemen, while the eastern part of Yemen is affected by ENE-WSW to WNW-ESE trending faults.

These periods of tectonic activity leave their structural impact on the rocks of the study area which are densely dissected by faults, dislocations and volcanic intrusions and resulted in a series of grabens, horsts and tilted fault blocks. The recorded fault trends in the study area are E-W, NE – SW, and SW – NE [4].

Based on the regional scale of fault movement (up throw/ down throw) three categories of faults were distinguished in the upper Wadi Rasyan area (including the area of study) by Dar El-Yemen [4], the three fault systems are:

- 1- E-W trending faults: including mainly two major faults (Taiz-Hajdah and Wadi Nakhlah- Habir) define the central graben. These two faults belong to category-I.
- 2- NW-SE trending faults: represented by a series of step faults at typically 0.5 to 3 km intervals downthrown to the west. Most faults of this system are of category-III.
- 3- NE-SW trending faults: including andesite dikes injected along faults are found to the north of Taiz. The most significant is the Ramadah-Wadi al-Haimah fault, which is considered the oldest fracture in the area. It shaped the area and regenerated during the Cretaceous and Tertiary. Faults of this system are generally short and belong to category-III except the Ramadah- Wadi al-Haimah fault which is of category-II.

However, smaller faults and joints follow the same trends of the major faults were also recorded but the most intensive faulting is in the NW-SE direction.

ACQUISITION AND INTERPRETATION OF GEOPHYSICAL DATA

In this study both vertical electrical resistivity sounding (VES) and ground magnetic survey techniques were used to study the groundwater aquifer conditions, such as the thickness of the Quaternary deposits, geological structures and the geometry of the groundwater aquifers.

I- Acquisition and interpretation of geoelectric resistivity data

A total of 15 vertical electrical soundings (VES) were analyzed and interpreted in this study. Nine soundings were conducted at Habeel Salman site "SI" inside and around the new campus of Taiz University and six soundings were conducted at Wadi Rudagah site "SII" (Fig. 1). The resistivity data was acquired by SAS 1000 resistivitymeter using Schlumberger configuration with maximum current electrodes separation (AB) vary between 400 and 1000 m. Due to natural obstacles, interruption by locals, cultivation and human activities, the current electrodes spacing at some VES's is very limited.

Results and Interpretation of resistivity data

To reduce the ambiguity associated with the interpretation of resistivity data, the observed apparent resistivity data was first manually interpreted using the conventional partial curve matching technique (utilizing master curves and the corresponding auxiliary curves) and later using the quantitative interpretation made using the IPI2WIN program to determine the thickness and resistivity of the different subsurface lithological units below each VES station. The resulted geoelectrical model from the program was then calibrated with the known lithology from the drilled wells in the studied sites. Figure (2) show examples of the obtained geoelectrical resistivity models at the two sites.

Qualitative interpretation includes comparison between the relative changes of apparent resistivity and thickness of the different layers. It gives information about the number of layers, their continuity and reflects the degree of homogeneity or heterogeneity of the layers.

In this study, the resistivity values of the first and second cycles of the resistivity curves at the two sites are characterized by HK, KH & AK, and QH types which reflect the heterogeneity of the surface and near surface layers due to the rapid variation in the moisture content and/or in the lithological composition of these layers between loose sediments, clay, sand and gravels with large boulders of massive rock blocks. All the field curves at both sites end with either H or K types, reflecting high

resistivity values (related to hard volcanic rocks or dry alluvium) or low resistivity values (related to saturated alluvium and/or fractured volcanic rocks), respectively.

a- Quantitative interpretation of resistivity data at Habel Salman site

The locations of the nine vertical electrical soundings conducted at Habel Salman site are shown in figure (4) and the parameters of the obtained resistivity models from these soundings are listed in table (1). This table shows that five geoelectrical layers were detected by VESs 1, 2, 3, 4, 6 and 7, and four geoelectrical layers by VESs 8 and 9, whereas VES 5 reflect six geoelectrical layers. The topmost layer has resistivity ranging between 16.9 Ω .m and 644 Ω .m and thickness varies from 0.8 m to 3.54 m. The large range of resistivity variation of this layer reflect varying in its composition from agricultural soil (at VESs 1, 6, 7 and 9) to dry loose surface sediments with boulders of massive rocks (at VESs 2, 3, 4, 5 and 8), the higher resistivity values occurs at places where large boulders of massive rocks (granite) are exposed on and/or near the ground surface, while the lower resistivity value (16.9 Ω .m) at VES 7 indicate wet to saturated soil layer. The resistivity of the second geoelectrical layer varies between 26.0 Ω .m – 272.0 Ω .m and thickness between 1.95 m – 13.3 m. This layer is generally vary from dry alluvium (at VESs 2, 3, 4, 8 and 9) to wet alluvium (at VESs 1, 5, 6 and 7). The third geoelectrical layer is characterized by resistivity values ranging between 12.6 Ω .m – 60.0 Ω .m and thickness varies from 2.63 m to 72.8 m. The nature of this layer varies from saturated alluvium (at VESs 2, 3, and 5) and saturated alluvium and weathered volcanics (at VESs 6, 8 and 9) to dry alluvium at (VESs 1, 4 and 7). This layer is considered as the main groundwater aquifer at shallow depths. The resistivity of the fourth geoelectrical layer varies between 5.1 Ω .m – 218 Ω .m and its thickness ranging between 32.2 m and 150 m. This layer is varying from saturated alluvium and weathered volcanics (at VESs 1 and 7), weathered highly fractured volcanics saturated by groundwater (at VESs 3 and 6), to moderately fractured and hard volcanics (at VESs 2, 4, 5, 8 and 9). The fifth geoelectrical layer is characterized by resistivity values ranging between 5.38 Ω .m – 149 Ω .m and it is encountered at depths vary between 44.85 m to 178.91 m, the resistivity values of this layer suggesting saturated alluvium and weathered volcanics (at VES 4), highly fractured volcanics saturated by groundwater (at VESs 2 and 5) and moderately fractured to massive volcanics (at VESs 1, 3, 6 and 7).

This layer represents the last detected geoelectric layer below all VESs except below VES 5, where a sixth geoelectric layer was encountered at depth of 197.6 m with resistivity of 56 Ω .m, suggesting hard volcanic rocks.

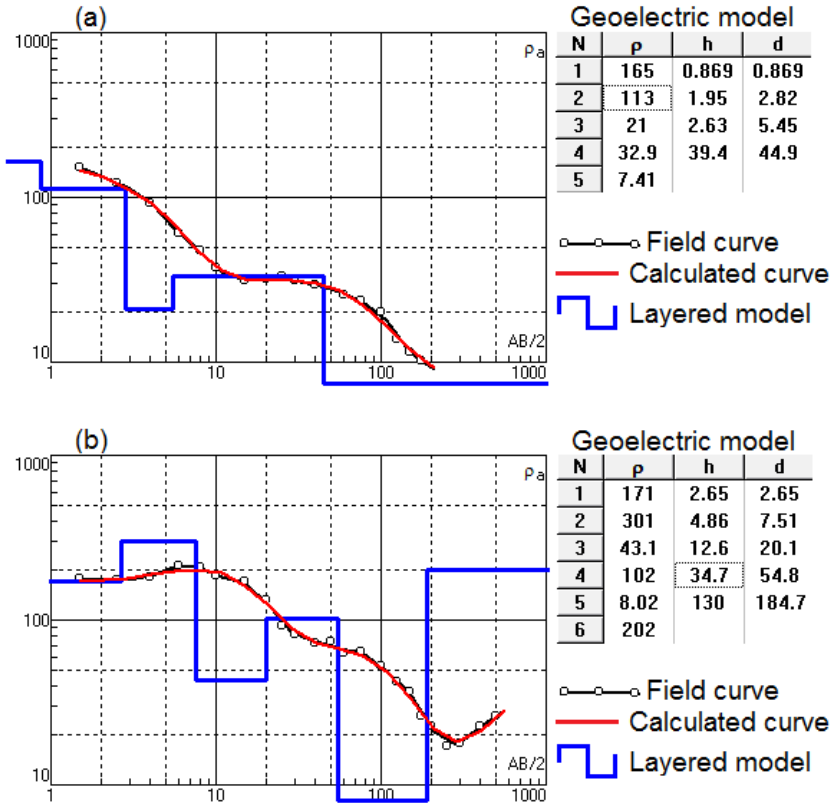


Figure 2: Interpretation results of (a) VES 4 at Habel Salman site and (b) VES 6 at Wadi Rudagah site.

Table 1: Resistivity and thickness of the detected geoelectrical layers obtained from interpretation of the VESs measured at Habel Salman and Wadi Rudagah sites

Site name	VES NO.	Layer No.											
		1		2		3		4		5		6	
		ρ $\Omega.m$	T (m)	ρ $\Omega.m$									
Habel Salman	1	55	0.9	26	4.17	60	20.8	10.5	139	41.9	-----	-----	
	2	353	2.4	237	9.31	14.1	14.4	43.1	45	6.06	-----	-----	
	3	326	1.2	194	4.67	25.1	21.4	5.06	32.2	149	-----	-----	
	4	165	0.9	113	1.95	21.0	2.63	32.9	39.4	7.41	-----	-----	
	5	198	3.5	27.2	13	14.6	28.4	35.3	72.5	5.38	80.2	56	
	6	68.9	1.5	42	6.14	16.1	72.8	7.36	57.9	58.4	-----	-----	
	7	16.9	1	36.2	13.3	56	14.6	9.02	150	39.8	-----	-----	
	8	644	1.4	272	4.16	12.6	68.5	63.1	-----	-----	-----	-----	
	9	41.6	0.8	179	6.65	17.5	52	218	-----	-----	-----	-----	
Wadi Rudagah	1	26.1	0.76	9.42	1.26	260	2.3	18.2	33.2	5.27	109	152	
	2	51.6	0.57	360	1.25	38.52	2.67	31.9	66.7	5.73	69.4	390	
	3	17.5	1.45	46.8	5.36	26.6	8.5	125	15	14.2	-----	-----	
	4	37.8	1.59	13.7	1.84	234	3.7	8.11	65.6	51.8	-----	-----	
	5	13.1	0.7	21	10.7	202	3.83	11.5	10.9	30.7	73.9	4.58	
	6	171	2.65	301	4.86	43.1	12.6	102	34.7	8.02	130	202	

T: Thickness of the geoelectric layers ρ : Resistivity of the geoelectric layers

Figure (3) is a geoelectrical cross-section extended through VESs 1, 2, 3, 4, 5 and 8 in the NW direction. This section shows the vertical and lateral extension of the detected geoelectric layers along the profile A-A' and indicates that the study area was affected by several faults resulted in the formation of several horsts and grabens.

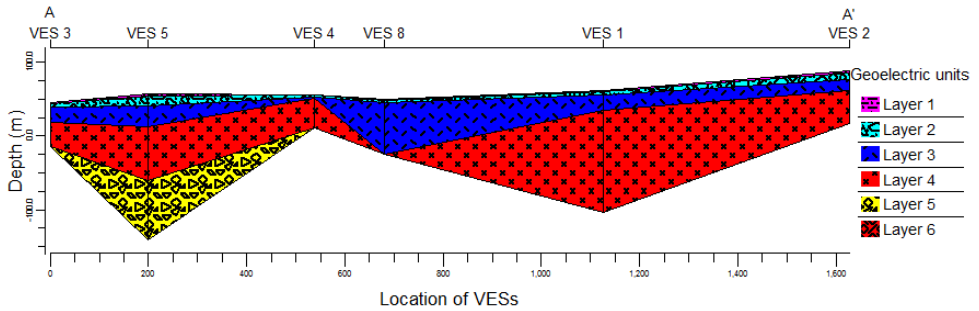


Figure 3: Geoelectrical cross-section through VESs 1, 2, 3, 4, 5 and 8 at Habel Salman site.

The above discussion indicates the existence of shallow and deep groundwater aquifers at the investigated site. The shallow aquifer was observed below VESs 2, 3, 4, 5, 6, 8 and 9 within the alluvium deposits and weathered volcanics at depths vary between 2.9 m and 16.5 m. The resistivity values of this aquifer vary between 12.6 Ω .m and 25.0 Ω .m, and its thickness varies from 2.7 m to 72.8 m.

The deep groundwater aquifer is located within the fractured volcanic rocks and recorded below VESs 2, 3, 4, 5 and 6 at depths ranging between 27.3 m and 117.4 m. This aquifer is characterized by resistivity values ranging between 5.06 Ω .m – 7.4 Ω .m. The thickness of this aquifer is ranging between 32.2 m and 80.2 m below VESs 3, 5 and 6 and undefined below VESs 2 and 4 since it represents the last detected layer below these sounding.

It is worth to mention here that the transitional zone between the shallow and deep aquifers was not detected below VESs 1, and 7 so that the detected saturated layers below these VESs were treated as shallow aquifer in figure (4) despite that there resistivity values (9.02 Ω .m – 10.5 Ω .m) fill the range between the upper and lower resistivity limits of the deep and shallow aquifers, respectively.

The variations of resistivity and thickness of the shallow groundwater aquifer are shown in figure (4a and b). this figure show gradual decreases in resistivity and increases in the aquifer thickness towards the central and western parts of the investigated site.

b- Quantitative interpretation of resistivity data at Wadi Rudagah site:

The distribution of the six vertical electrical soundings conducted at Wadi Rudagah site are shown in figures (6) and their results are summarized in table (1). The obtained geoelectrical resistivity models at this site reflect six geoelectric layers at VESs 1, 2, 5, and 6 and five geoelectric layers at VESs 3 and 4. An example of these geoelectrical resistivity models is shown in figure (2b). The top geoelectric layer is characterized by resistivity values ranging between 13.1 Ω .m and 171 Ω .m, the maximum resistivity value (171 Ω .m) was recorded at VES 6 indicating loose surface deposits, whereas the recorded resistivity at the remaining VESs fill the range 13.1 Ω .m – 51.6 Ω .m indicating agricultural soil. This layer extended downward from the ground surface to a depth varies between 0.57 m and 2.65 m.

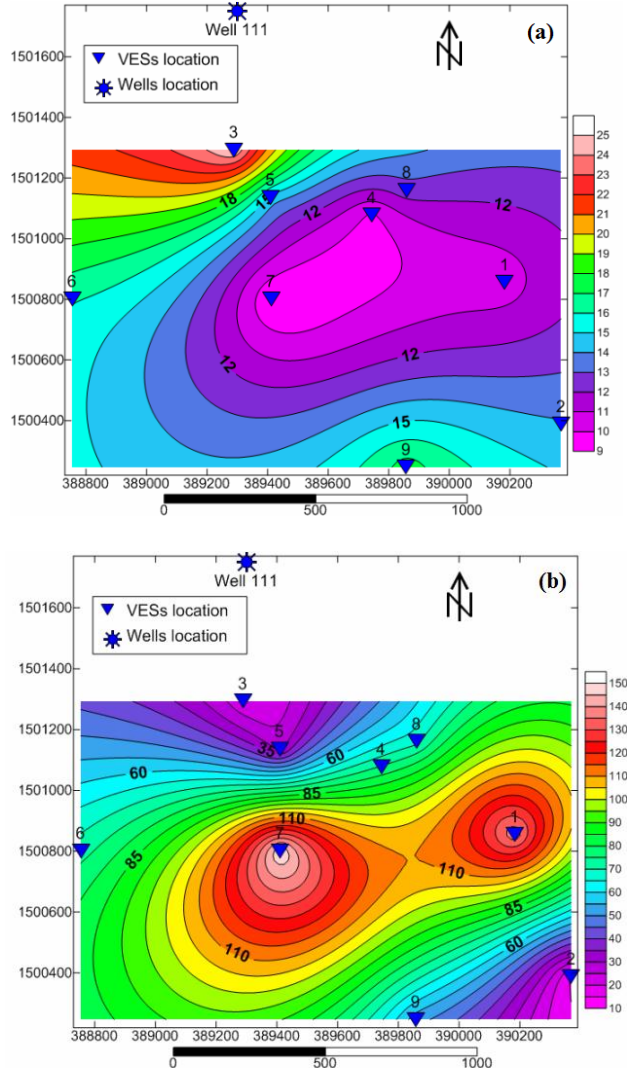


Figure (4) Variations of (a) resistivity and (b) thickness of the shallow groundwater aquifer at Habel Salman site.

The second geoelectric layer is characterized by resistivity values ranging from 9.42 Ω .m to 360 Ω .m and with thickness vary from 1.25 m to 10.7 m. The higher resistivity values recorded at VESs 2 and 6 suggesting change of layer composition from agricultural soil (at VESs 1, 3, 4 and 5) to sand, gravel with boulders of massive rocks (at VESs 2 and 6). The third geoelectrical layer has resistivity values ranging between 26.6 Ω .m and 260 Ω .m and thickness ranging between 2.3 m and 12.6 m. The large variations of resistivity indicate change in the layer composition

from dry and wet clay and silt (at VESs 2, 3, and 6) to dry sand, gravel and boulders of massive rocks (at VESs 1, 4, and 5). The fourth geoelectrical layer has resistivity values vary from 8.1 $\Omega\cdot\text{m}$ to 125 $\Omega\cdot\text{m}$ indicating wet to saturated alluvium and weathered volcanics (at VESs 1, 2, 4, and 5) and dry alluvium deposits (at VESs 3 and 6). The thickness of this geoelectrical unit varies between 10.9 m and 66.7 m. The fifth geoelectrical unit is characterized by resistivity values ranging between 5.27 $\Omega\cdot\text{m}$ and 51.8 $\Omega\cdot\text{m}$ indicating saturated fractured volcanics at VESs 1 and 2 (5.25 $\Omega\cdot\text{m}$ – 5.73 $\Omega\cdot\text{m}$), saturated alluvium and/or weathered volcanics at VESs 3 and 6 (8.02 $\Omega\cdot\text{m}$ – 14.2 $\Omega\cdot\text{m}$) and wet to dry alluvium at VESs 4 and 5 (30.7 $\Omega\cdot\text{m}$ – 51.8 $\Omega\cdot\text{m}$). The thickness of this layer varies from 69.4 m to 130 m below VESs 1, 2, 5 and 6 and undefined below VESs 3 and 4.

The sixth geoelectrical layer was encountered at depths vary between 140.6 m and 184.8 m (at VESs 1, 2, and 6) with resistivity values ranging between 152 $\Omega\cdot\text{m}$ to 390 $\Omega\cdot\text{m}$ indicating hard volcanics. Below VES 5, this layer was encountered at depth of 100 m with resistivity of (4.58 $\Omega\cdot\text{m}$) indicating saturated fractured volcanics.

Figure (5) is a geoelectrical resistivity cross-section extended from the north to the south through the six soundings (VESs 1 to 6). This figure reflects both the vertical and lateral variations in the thickness of the detected geoelectric layers at this site as well as the faults affecting the area and resulted in the formation of several horsts and grabens.

The analysis of the VESs results pointing to the existence of two groundwater aquifers. The shallow aquifer is recorded below VESs 1, 3, and 5 within the alluvium deposits and weathered volcanics at depths vary between 4.3 m and 15.2 m, with resistivity values vary between 11.5 $\Omega\cdot\text{m}$ and 18.2 $\Omega\cdot\text{m}$ and its thickness ranging between 10.9 m and 33.2 m (below VESs 1 and 5) and undefined below VES 3. The deep aquifer is recorded below VESs 1, 2 and 5 at depths vary from 37.52 m to 71.19 m. It is characterized by resistivity values of less than 6.0 $\Omega\cdot\text{m}$ and by thickness varies between 69.4 m and 109 m (below VESs 1 and 2) and undefined below VES 5. The depth and thickness of this aquifer indicates that it is mainly consists of fractured volcanics.

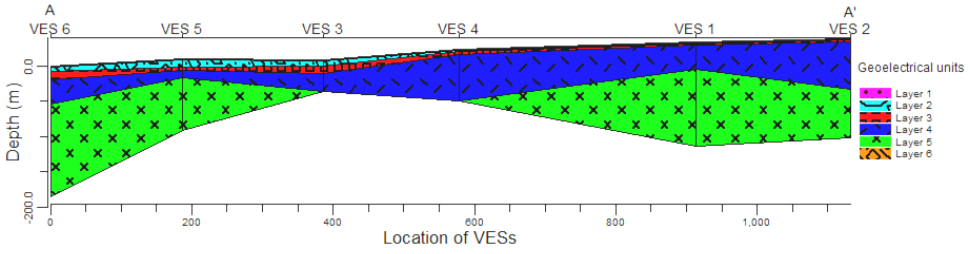


Figure 5: Goelectrical cross-section through VESs 1 - 6 at Wadi Rudagah site.

As noted at Habel Salman site, the transitional zone between the two aquifers was also not recorded below VESs 4 and 6 at this site, so that the detected saturated layers below these VESs were treated as shallow aquifer (Fig. 6a) despite that there resistivity values (8.02 Ω .m and 8.11 Ω .m) lie between the upper and lower resistivity limits of the deep and shallow aquifers respectively.

As shown in figure (6a) the resistivity of the shallow aquifer increases gradually from the west to the east whereas the thickness of the aquifer (Fig. 6b) increases toward the north of the mapped area.

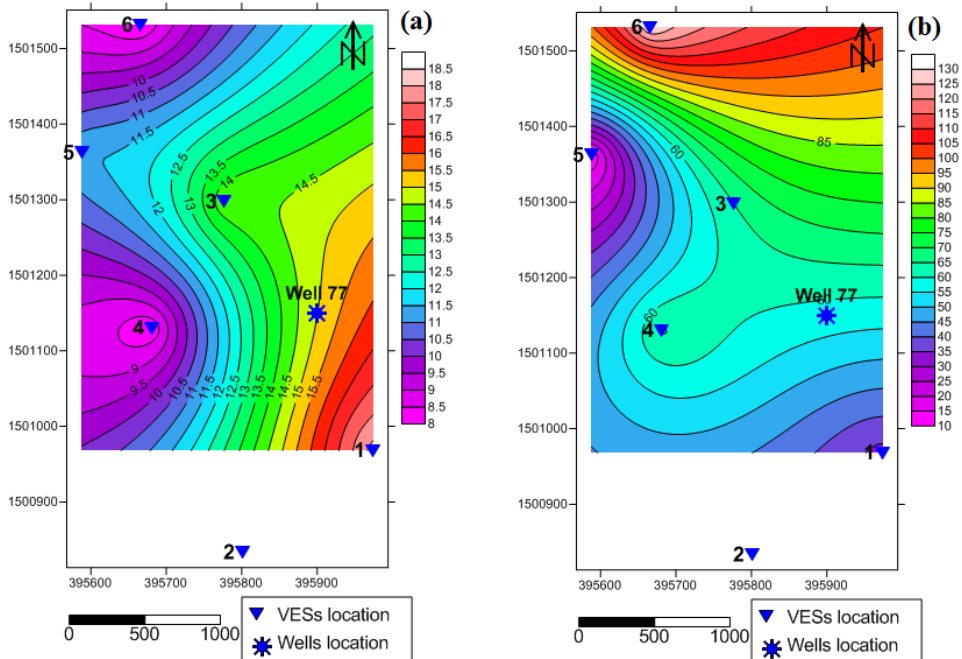


Figure 6: Variations of (a) resistivity and (b) thickness of the shallow groundwater aquifer at Wadi Rudagah site.

II- Acquisition, processing and interpretation of the ground magnetic data

Al Hawjalah area is located in the northern part of Taiz City and contain one of the well fields that supply the city by water. This area of study was divided into two locations (A and B) separated by the asphalt road connecting between Taiz city and Al-Mikhlaf villages. Due to the effect of topography and/or human activities, the ground magnetic survey was conducted along irregular grids distributed through the main valley and its tributaries at this site.

Ground magnetic data were collected using proton precession magnetometer and gradiometer (PMG1) with a resolution of 0.1 nT and absolute accuracy of ± 1 nT.

The total intensity of the earth's magnetic field was measured along irregular grids with sampling intervals of 100 m and lines separation of 200 m. The geomagnetic field was measured by setting the sensor at 2.0 m height above the ground level with the north mark on the sensor was kept to point to the geographical north. A single magnetometer was used in the survey and therefore the base station was reoccupied every one hour.

The total magnetic intensity measurements were subjected to diurnal corrections and the IGRF value (37468.4 nT) was subtracted from the readings of the whole survey stations. The final result is a total intensity magnetic maps at locations "A" and "B" (Fig. 7).

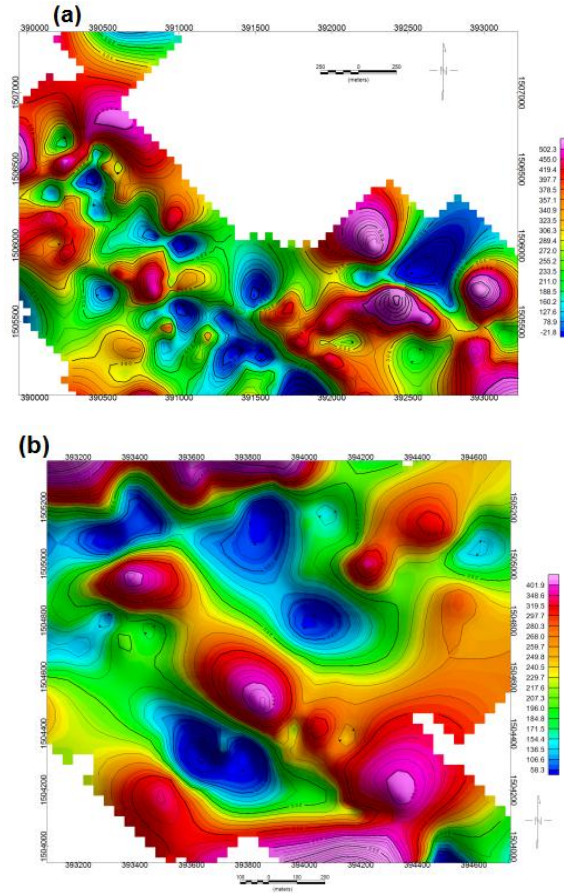


Figure 7: Total intensity magnetic anomaly maps of (a) location “A” and (b) location “B” at Al Hawjalah site.

To eliminate the shape distortion of magnetic anomalies due to the effect of inclination and declination of the earth’s magnetic field at low latitude areas, the total magnetic intensity data were reduced to the magnetic pole by using geosoft software and the obtained reduced to the pole magnetic anomaly maps (RTP) are shown in figure (8).

The RTP map of location “A” (Fig. 8a) is dominated by high magnetic anomaly closures oriented in the NW-SE, NE-SW and E-W directions with maximum amplitude of 760 nT while the magnetic low anomalies occur in the form of isolated elongated to rounded closures oriented mainly in the N-S, NE-SW and NW-SE directions with minimum amplitude of -300 nT.

At location “B”, the RTP map (Fig. 8b) is dominated by high anomaly closures oriented NW-SE, NE-SW, and E-W with maximum amplitude of 580 nT, whereas the low magnetic anomalies are occur in the form of elongated closures oriented NW-SE, NE-SW and E-W, with minimum value of -100 nT recorded in the elongated low magnetic anomaly closure at the upper western corner of the map.

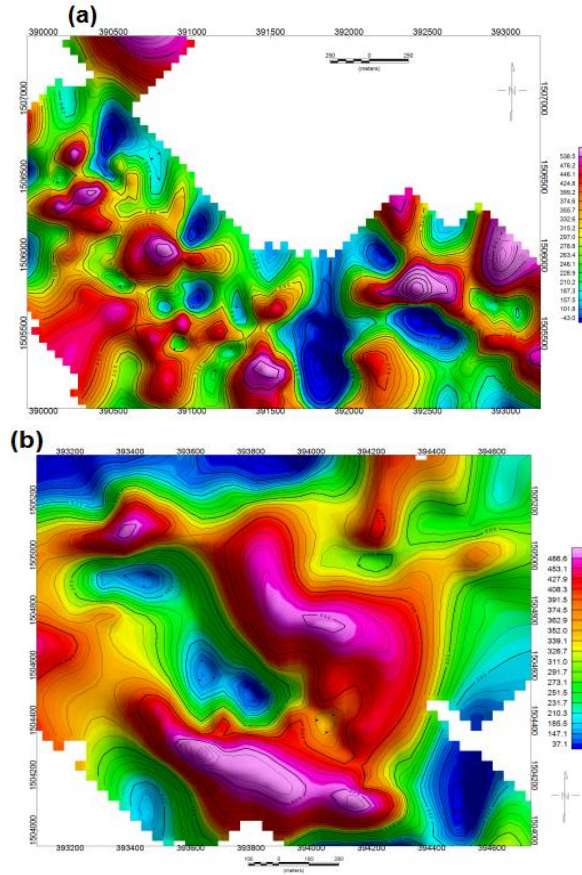


Figure 8: Reduced to the pole magnetic anomaly maps of (a) location “A” and (b) location “B” at Al Hawjalah site.

The RTP maps were subjected to spectrum analysis to define and separate the frequency components of the shallow and deep anomaly sources at the two locations (A and B). The band-pass filter technique with the cut off parameters obtained from the two dimensional power spectrum plots was used to separate the shallow and deep anomaly sources.

The local and regional magnetic anomaly maps of location “A” (Fig. 9) were obtained using the cut off parameters $3.87 \leq k \leq 8.25$ and

$0.25 \leq k \leq 3.87$ cycle/km, respectively. Whereas the cut off parameters of the band-pass filters that used to separate the shallow and deep magnetic anomalies at location “B” (Fig. 10) are $3.92 \leq k \leq 11.2$ and $0.009 \leq k \leq 3.92$ cycle/km, respectively.

The local magnetic anomaly map of location “A” (Fig. 9a) shows alternated belts of interconnected elongated to rounded positive and negative magnetic anomalies oriented in the NW-SE, NNW-SSE, WNW-EES, E-W and NE-SW directions with amplitudes vary between 40 nT and -60 nT.

On the other hand, the regional magnetic anomaly map of location “A” (Fig. 9b) is characterized by positive magnetic anomaly features oriented in the NW-SE, NE-SW and E-W directions with maximum amplitude of 400 nT. The negative magnetic anomaly features occur in the form of elongated to rounded closures separating the positive ones and oriented mainly in the N-S, NE-SW and NW-SE directions with minimum amplitude of -600 nT. This map is very similar to the RTP map (Fig. 8a) both in the distribution and orientation of the high and low magnetic anomalies.

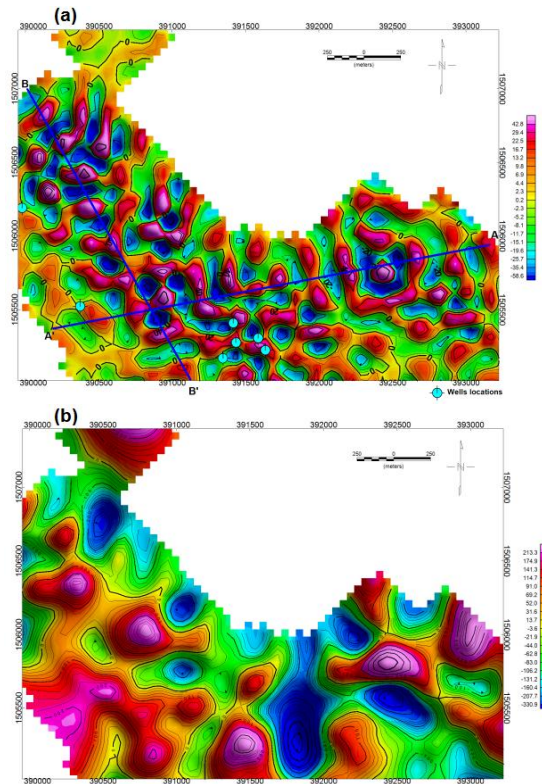
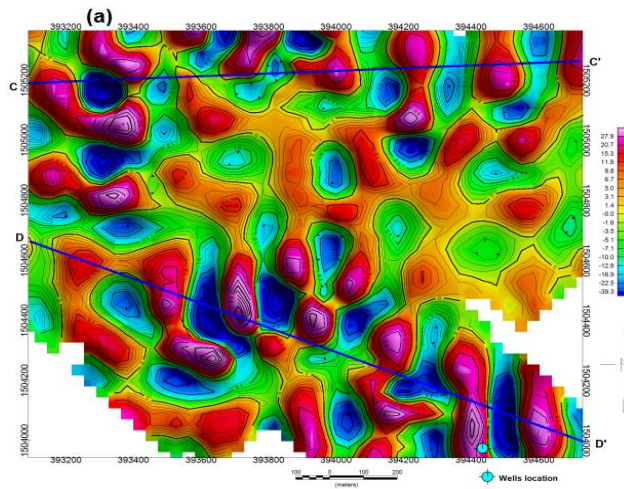


Figure 9: local (a) and regional (b) magnetic anomaly maps of Al Hawjalah site (location A).

At location “B”, the shallow magnetic anomaly map (Fig. 10a) is dominated by alternation of elongated to rounded positive and negative magnetic anomalies oriented N-S, NNW-SSE, NW-SE, NE-SW and E-W with amplitude values vary between 100 nT and -80 nT. The amplitude of the magnetic anomalies in the southern, northern and western parts are higher than those in the eastern and central parts of the map indicating that the volcanic rocks are exposed at the surface or the thickness of the alluvium deposits in the southern, northern and western parts is smaller than that in the other parts of the mapped area. The pattern of the regional magnetic anomaly map of location “B” (Fig. 10b) is very similar to the RTP map of this location (Fig. 8b), but they differs in the amplitude of these anomalies which is in this map varies from 240 nT to 300 nT.

The great similarity between the regional and RTP maps of the two locations (A and B) reveals that the contribution of the overburden to the geomagnetic field in the area of study is totally absent or at least insignificant. Also the local and regional structure are mainly extending in both NW - SE and NNE – SSW directions.



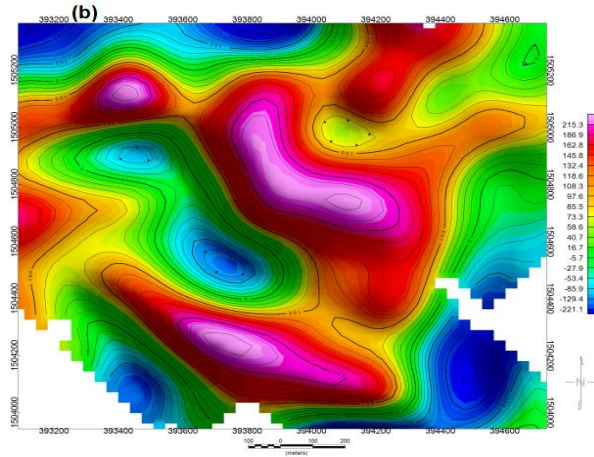


Figure 10: local (a) and regional (b) magnetic anomaly maps of Al Hawjalah site (location B).

To understand better the configuration and structural framework of the Quaternary aquifer in the area under investigation, a two dimensional modeling technique was conducted by using GM-SYS software along profiles A-A' and B-B' at location "A" (Fig. 9a) and profiles C-C' and D-D' at location "B" (Fig. 10a). The magnetic intensity along these profiles was traced and used as the observed values. The magnetic field was calculated iteratively by assuming the magnetic susceptibility of the Quaternary deposits to be 0.0 and testing several values for the magnetic susceptibility of the volcanic rocks until good fits were reached between the observed and the calculated profiles. The magnetic susceptibility of the volcanic rocks at which the best fitting along the four profiles was obtained ranges between 0.0067 – 0.0074 cgs.

Profile A–A' cuts across the northern portion of location "A" in the EEN-WWS direction. The two dimensional modeling along this profile (Fig. 11a) indicates that the area was affected by normal faults with different throws and dip angles resulted in the formation of several grabens and horsts. The recorded thickness of the overburden along this profile varies between 15 m and 50 m and decreases in the EEN direction.

Profile B-B' is extended in the NW-SE direction throughout the western part of location "A". The 2D model of this profile (Fig. 11b) reflects alternation of grabens and horsts resulted by several normal faults with different throws. The thickness of the alluvial deposits ranging from 8.0 m to 114.6 m and increases in the NE direction.

Profile C-C' cuts across the northern part of location "B" in the E-W direction. The 2-D model along this profile (Fig. 12a) indicates successive graben and horst like structures with depth ranges between 3.0 m (at the NW end of the profile) and 111.0 m (near the SE end of the profile).

Profile D-D' is oriented in the NW-SE direction. The basement surface along this profile is characterized by up-lifted and down-lifted blocks resulted in the formation of several horsts and grabens (Fig. 12b). The minimum thickness of the alluvium deposits (16 m) was recorded at the SW end of the profile while the maximum thickness of this layer (73 m) was recorded at the NE end of the profile.

The above analysis of magnetic data indicates that the area was affected by periods of tectonic activity resulted in a complex structural pattern represented mainly by intense faulting leading to the formation of successive grabens and horsts with different lengths, depths and orientations.

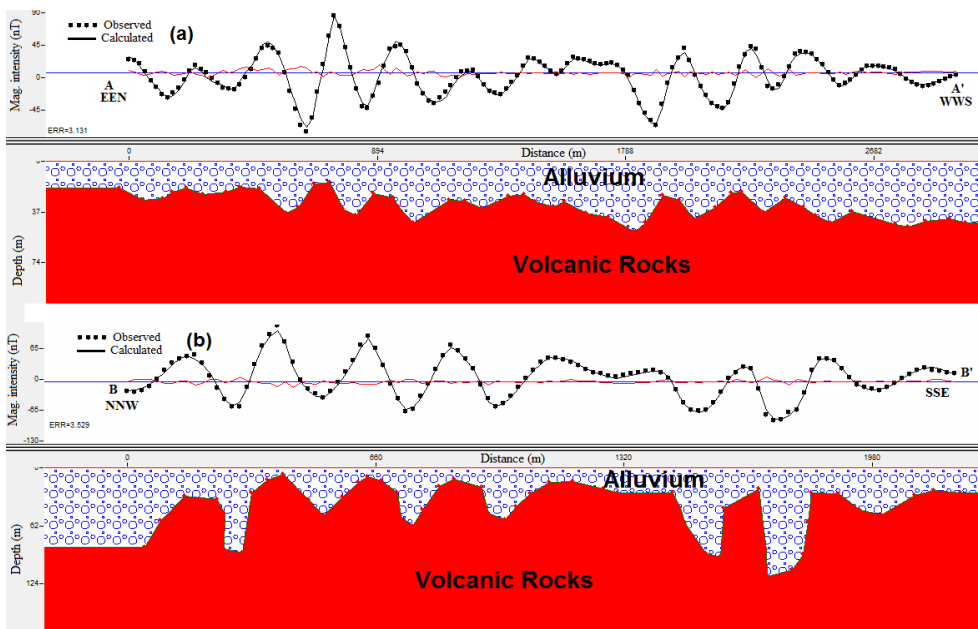


Figure 11: Two-dimensional modeling along (a) profile A-A' and (b) profile B-B' at Al Hawjalah site (location A).

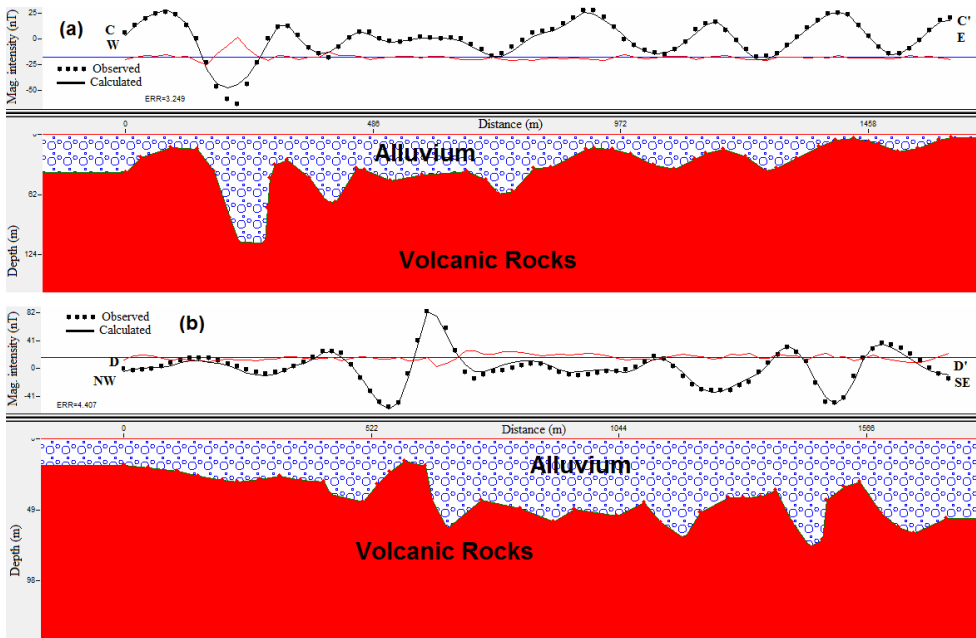


Figure 12: Two-dimensional modeling along (a) profile C-C' and (b) profile D-D' at Al Hawjalah site (location B).

The local authority of Taiz governorate planned to solve partially the acute shortage of drinking water in Taiz city by developing the groundwater aquifers inside and around the city by increasing their recharge through a rainwater harvesting project. To provide information that will be valuable for this project, the lineaments on the residual and regional magnetic maps of Al Hawjalah aquifer (at the two locations A and B) were traced, analyzed and presented in the form of rose diagrams and structural lineaments map (Figs. 13 and 14). Generally, the magnetic lineaments reflects either geologic structures and/or contacts between rock units with different magnetic susceptibility, consequently the study and analysis of magnetic lineaments distribution on and below the ground surface and correlating them with the distribution of the geological faults and joints is of great important in the study of groundwater potentiality and also in the development of groundwater aquifers to meet the good conditions of the aquifer recharge.

The traced geological faults in the area of study trending in the NW-SE and NE-SW directions (Fig. 14), while the magnetic lineaments trending mainly in the NW-SE, NE-SW, and E-W directions for shallow magnetic map and in the NW-SE and NE-SW directions for deep magnetic anomaly maps (Figs. 13 and 14). The general trend of the traced

magnetic lineaments from the shallow and deep magnetic maps is in general agree to a great extent with the above mentioned trends of the three faults categories recorded in the upper Wadi Rasyan area (including Al Hawjalah site in this study) by Dar El-Yemen [4].

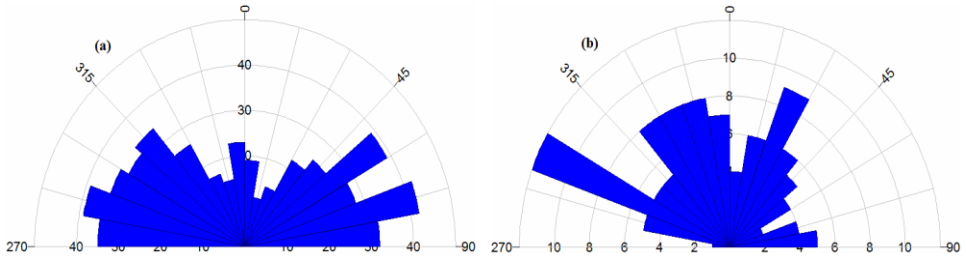


Figure 13: Rose diagrams of the lineaments traced from the local (a) and regional (b) magnetic anomaly maps at locations A and B.

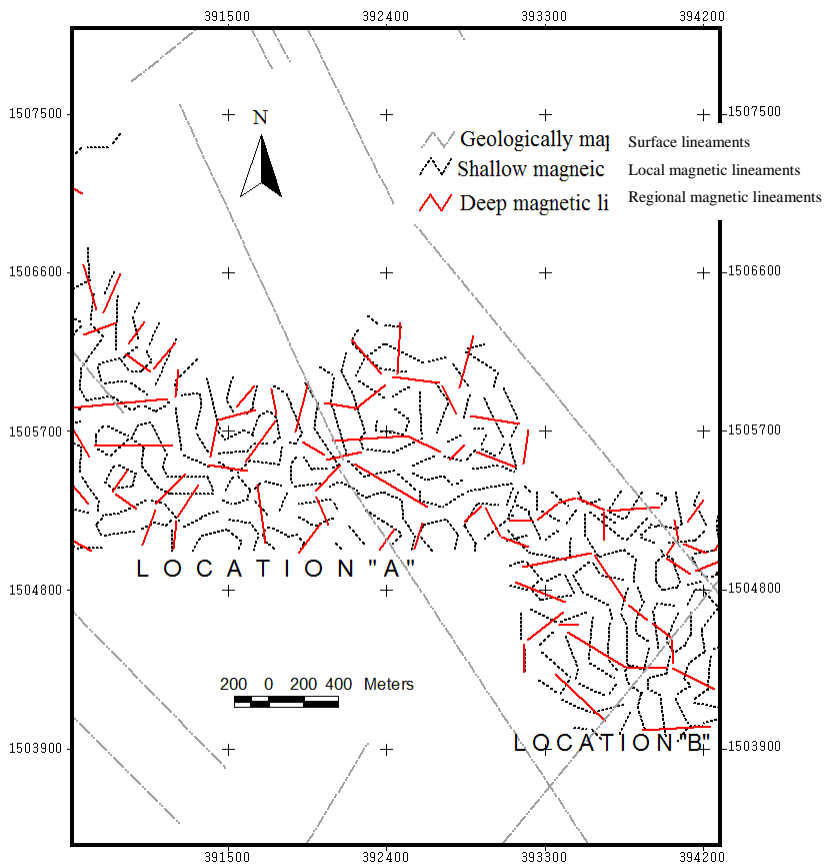


Figure 14: Structural lineament map traced from geological map and from shallow and deep magnetic anomaly maps at Al Hawjalah site.

CONCLUSIONS

The vertical electrical sounding survey at Habeel Salman and Wadi Rudagah sites (sites I and II, respectively) revealed the existence of two groundwater aquifers. The shallow aquifer consists of Quaternary deposits and weathered volcanic rocks and detected at depths vary between 5.56 m and 16.50 m at Habeel Salman site and between 1.82 m and 44.31 m at Wadi Rudagah site. The thickness of this aquifer ranging from 14.50 m to 72.8 m (with resistivity values in the range of 12.6 to 25.0 Ω .m) at Habeel Salman site and from 2.67 m to 65.6 m (with resistivity values ranging between 2.67 Ω .m and 18.2 Ω .m) at Wadi Rudagah site.

The deep aquifer consists mainly of fissured volcanic rocks and recorded at depths vary between 27.3 m and 117.4 m at Habeel Salman site and between 37.51 m and 100 m at Wadi Rudagah site. The thickness of this aquifer ranging from 24.5 m to 139 m (with resistivity less than 8.0 Ω .m) at Habeel Salman site and from 69.4 m to 130 m (with resistivity less than 6.0 Ω .m) at Wadi Rudagah site. The transitional zone between these aquifers was not recorded below some VESs both at Habeel Salman and Wadi Rudagah sites hence the aquifer below these VESs was treated as shallow aquifer.

On the other hand, the ground magnetic survey at Al-Hawjalah site indicates that the thickness of the shallow aquifer (overburden layer) varies between 3.0 m and 114.6 m. This aquifer is structurally controlled by several faults affecting the area and resulted in the formation of a series of grabens and horsts with different depths trending mainly in the NW-SE, NE-SW and E-W directions.

ACKNOWLEDGMENTS

The author would to express his deep thanks to the National Water Resources Authority (NWRA), Taiz branch and also to the Taiz Water and Sanitation Local Corporation (TWSLC) for providing us by the required wells data and previous studies.

REFERENCES

- [1] Glass N. (2010) The Water Crisis in Yemen: Causes, Consequences and Solutions. *Global Majority E-Journal* 1 (1), 17-30.
 - [2] Khanbari Khalid and Huchonc Philippe (2010) Paleostress analysis of the volcanic margins of Yemen; *Arab. J. Geosciences*, 3, 529-538.
 - [3] Mezhelovsky N.V., Rybakov V. S. , Saif A. S., Emad M. and Mezhelovsky I. N. (1997) Groundwater studies wadis Al Ghayl, Bani Khawlan and Warazan. Final report Contract NWRA/YEM/97/200-02 V. I: Main report, 116 pp.
 - [4] Dar El-Yemen Consultants, 1997. Hydrogeological and land-use studies in the Ta'iz region (Upper Wadi Rasyan). Vol.I: Main report. Volume II: Annexes.
 - [5] Kruck W. and Schaffer U. (1991) Geological map of the Republic of Yemen, Sheet: Taiz, 1: 250000. (Republic of Yemen). Federal Institute of Geosciences and Natural Resources, Hanover, Germany.
 - [6] Capaldi G, Chiesa S, Manetti P, Orsi G, Poli G (1987) Tertiary anorogenic granites of the western border of the Yemen Plateau. *Lithos* 20, 433-444.
 - [7] Chazot G, Bertrand H (1995) Genesis of silicic magmas during Tertiary continental rifting in Yemen. *Lithos* 36, 69-84.
 - [8] Ellis AC, Kerr HM, Cornwell CP, Williams DO (1996) A tectono-stratigraphic framework for Yemen and its implications for hydrocarbon potential. *Petroleum Geoscience* 2, 29-24.
 - [9] Brannan J, Sahota G, Gerdes KD, Berry JAL (1999) Geological Evolution of the Central Marib-Shabwa Basin, Yemen. *GeoArabia* 4 (1), Gulf PetroLink, Bahrain.
 - [10] Schüppel D, Wienholz R (1990) The development of Tertiary in the Habban-Al Mukalla area, PDR Yemen. *Z. geol. Wiss., Berlin* 6, 523-528.
 - [11] Watchorn F, Nichols GJ, Bosence DWJ (1998) Rift-related sedimentation and stratigraphy, southern Yemen (Gulf of Aden). In "Sedimentation and tectonics in the Rift Basins Red Sea-Gulf of Aden". B. Purser and D. Bosence, Eds. Chapman et Hall, London. 165-189.
 - [12] Ziegler MA (2001) Late Permian to Holocene paleofacies evolution of the Arabian plate and its hydrocarbon occurrences. *GeoArabia* 6 (3), 445-503.
-

تطبيقات الحسابات الكهربية الراسية والمسح المغناطيسى الأرضى لإستكشاف المياه الجوفية فى المنطقه المحيطة بمدينة تعز- اليمن

أمين نعمان القدسى

قسم الجيولوجيا- كلية العلوم- جامعة تعز- اليمن

اجريت هذه الدراسة على مناطق حبيل سلمان، و وادى الرداغا و الحويجه التى تقع غرب و شرق و شمال مدينة تعز حيث تم إجراء خمسة عشر جسه كهريبيه رأسيه بمنطقتى حبيل سلمان و وادى الرداغا بإستخدام ترتيب شلمبرجير بينما اجرى عمل مسح مغناطيسى أرضى بمنطقة الحويجه والتى تحتوى على مجال واعد لمد المدينه بالمياه.

و قد أوضحت النتائج المستخلصه من الدراسة عن وجود خزائين للماء يكون العلوى أقرب إلى سطح الارض ويتكون من رواسب حديثه يغلب عليها الفتات البركانى، بينما يتواجد الخزان السفلى الأعمق خلال الفوالق والكسور الضاربة فى الصخور البركانيه.

وفى أثناء حقبه السينوزوك نجد أن هذه الخزانات قد تأثرت بعديد من الفوالق نتيجة لإنبثاق بركانيات اليمن الشهيره و كذلك تكوين كلا من البحر الاحمر وخليج عدن اللذان أديا إلى تكوين مجموعة متتالية من المنخفضات و المرتفعات.